Propulsion and Power Research 2015;4(1):50–62

HOSTED BY

ELSEVIER

http://ppr.buaa.edu.cn/

Propulsion and Power Research

www.sciencedirect.com

ORIGINAL ARTICLE

Study of heat transfer and flow of nanofluid in permeable channel in the presence of magnetic field

M. Fakour[a,*], A. Vahabzadeh[a], D.D. Ganji[b]

[a]Young Researchers and Elites Club, Sari Branch, Islamic Azad University, Sari, Iran
[b]Department of Mechanical Engineering, Sari Branch, Islamic Azad University, Sari, Iran

Received 6 October 2014; accepted 21 January 2015
Available online 1 April 2015

KEYWORDS

Least square method (LSM);
Laminar viscous flow;
Heat transfer;
Uniform magnetic field;
Channel with porous walls

Abstract In this paper, laminar fluid flow and heat transfer in channel with permeable walls in the presence of a transverse magnetic field is investigated. Least square method (LSM) for computing approximate solutions of nonlinear differential equations governing the problem. We have tried to show reliability and performance of the present method compared with the numerical method (Runge-Kutta fourth-rate) to solve this problem. The influence of the four dimensionless numbers: the Hartmann number, Reynolds number, Prandtl number and Eckert number on non-dimensional velocity and temperature profiles are considered. The results show analytical present method is very close to numerically method. In general, increasing the Reynolds and Hartman number is reduces the nanofluid flow velocity in the channel and the maximum amount of temperature increase and increasing the Prandtl and Eckert number will increase the maximum amount of theta.

1. Introduction

Flow problem in a porous tube or channel received much attention in recent years due to its various applications in medical engineering, for example, in the dialysis of blood in artificial kidney [1], in the flow of blood in the capillaries [2], in the flow in blood oxygenators [3], as well as in many

*Corresponding author. Tel.: +989119579177.

E-mail addresses: mehdi_fakour@yahoo.com; mehdi_fakoor8@yahoo.com (M. Fakour); vahabzadeh_a@yahoo.com (A. Vahabzadeh); ddg_davood@yahoo.com (D.D. Ganji).

Peer review under responsibility of National Laboratory for Aeronautics and Astronautics, China.

http://dx.doi.org/10.1016/j.jppr.2015.02.005

Nomenclature

LSM	least square method
NUM	numerical method
P	pressure
q	mass transfer parameter
Re	Reynolds number
U	dimensionless velocity in the x direction
V	dimensionless velocity in the y direction
h	suspension height
Ec	Eckert number
Ha	Hartmann number
Pr	Prandtl number
L_x	length of the slider
C_p	specific heat
k	thermal conductivity
$\Delta T = T_h - T_0$	difference temperature between the plates
α	fluid thermal diffusivity
u_0	x velocity of the pad
u	dimensionless x-component velocity
v	dimensionless y-component velocity
u^*	velocity component in the x direction
v^*	velocity component in the y direction
x	dimensionless horizontal coordinate
y	dimensionless vertical coordinate
x^*	distance in the x direction parallel to the plates
y^*	distance in the y direction parallel to the plates

Greek symbols

ρ	fluid density
θ	dimensionless temperature
ν	kinematic viscosity
σ	electrical conductivity
ε	aspect ratio h/L_x

other engineering areas such as the design of filters [4], in transpiration cooling boundary layer control [5] and gaseous diffusion [6]. In 1953, Berman [7] described an exact solution of the Navier-Stokes equation for steady two-dimensional laminar flow of a viscous, incompressible fluid in a channel with parallel, rigid, porous walls driven by uniform, steady suction or injection at the walls. This mass transfer is paramount in some industrial processes. More recently, Chandran and Sacheti [8] analyzed the effects of a magnetic field on the thermodynamic flow past a continuously moving porous plate.

Slow viscous flow problem in a semi-porous channel in the presence of transverse magnetic field is investigated by Sheikholeslami et al. [9]. They show that the method is asymptotically optimal Homotopy a powerful method for solving nonlinear differential equations, such as the problem. Soleimani et al. [10] studied of natural convection heat transfer in an enclosure filled mid-loop with nanofluid using the control volume based finite element method. They founded turn angle has a significant effect on flow lines, isotherms and local Nusselt number is maximum or minimum values. Sheikholeslami et al. [11] investigated the flow of nanofluid and heat transfer characteristics between two horizontal plates in a rotating system. Their results showed that for suction and injection, the heat transfer rate increases with the nanoparticle volume fraction, Reynolds number, and parameter injection/suction increases and then decreases with the strength of the spin parameter. Steady magneto hydrodynamic free convection boundary layer flow past a vertical semi-infinite flat plate embedded in water filled with a nanofluid has been theoretically studied by Hamad et al. [12]. They found that copper and silver nanoparticles have proved that the highest cooling performance for this problem. Natural convection of a non-Newtonian copper-water nanofluid between two infinite parallel vertical flat plates was investigated by Domairry et al. [13]. They concluded that as the size of nanoparticles increases, the boundary layer thickness increases, the thermal boundary layer thickness decreases. Sheikholeslami et al. [14] studied the natural convection in a concentric annulus between a cold outer square and heated inner circular cylinders in the presence of static radial magnetic field. Sheikholeslami et al. [15] performed a numerical analysis for natural convection heat transfer of Cu-water nanofluid in a cold outer circular enclosure containing a hot inner sinusoidal circular cylinder in the presence of horizontal magnetic field using the control volume based finite element method. They concluded that in the absence of a magnetic field, increasing the Rayleigh number increases, while the opposite trend was observed in the presence of a magnetic field decreases. Sheikholeslami et al. [16] studied the effects of magnetic field and nanoparticle on the Jeffery-Hamel flow using adomian decomposition method. They showed that increasing Hartmann number will lead to backflow reduction. Recently several authors investigated about nanofluid flow and heat transfer [17–25]. There are some simple and accurate approximation techniques for solving nonlinear differential equations called the weighted residuals methods (WRMs). Collocation, Galerkin and least square method (LSM) are examples of the WRMs which are introduced by Ozisik [26] for using in heat transfer problem. These methods have been successfully applied to solve many types of nonlinear problems [27–32].

The main goal of this paper is to examine the laminar nanofluid flow in channel with permeable walls in the presence of transverse magnetic field using least square method. Effective volume fraction nanofluid, Hartmann number, Reynolds number, Prandtl number, and Eckert number on the velocity and temperature considered. In addition to speed and temperature for different structures nanofluid (copper and silver nanoparticles in water or ethylene glycol) depicted. In general, increasing the Reynolds and Hartman number is reduces the nanofluid flow velocity in the channel and the maximum amount of temperature increase and increasing the Prandtl and Eckert number will increase the maximum amount of theta.

2. Problem description

Steady two-dimensional laminar flow of an incompressible viscous electrically conducting fluid in a channel with permeable walls with a long rectangular plate with uniform translation in x^*, L_x over an infinite porous plate and made to consider. The distance between the two plates is h. Suction of fluid through the permeable walls is done with speed q, where for $q>0$, the suction is concerned. (Figure 1). A uniform magnetic field B is assumed to be applied towards direction y^* (Figure 2).

In the case of a short circuit to neglect the electrical field and perturbations to the basic normal field and without any gravity forces, the governing equations are [33,34]:

$$\frac{\partial u^*}{\partial x^*}+\frac{\partial v^*}{\partial y^*}=0, \tag{1}$$

$$u^*\frac{\partial u^*}{\partial x^*}+v^*\frac{\partial u^*}{\partial y^*} = -\frac{1}{\rho_{nf}}\frac{\partial P^*}{\partial x^*}+\nu_{nf}\left(\frac{\partial^2 u^*}{\partial x^{*2}}+\frac{\partial^2 u^*}{\partial y^{*2}}\right)-u^*\frac{\sigma_{nf}B^2}{\rho_{nf}}, \tag{2}$$

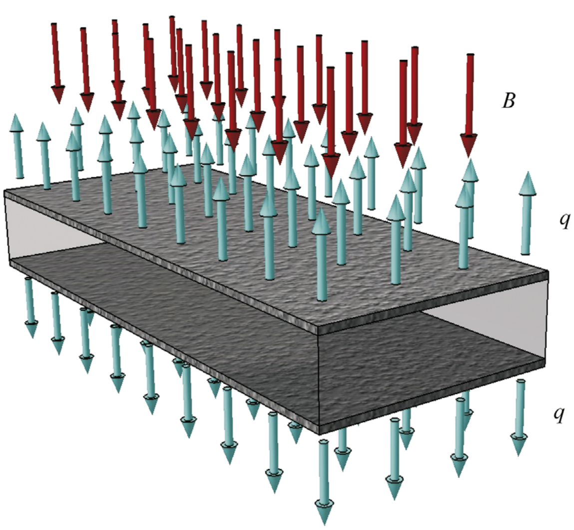

Figure 1 Three-dimensional schematic of the problem.

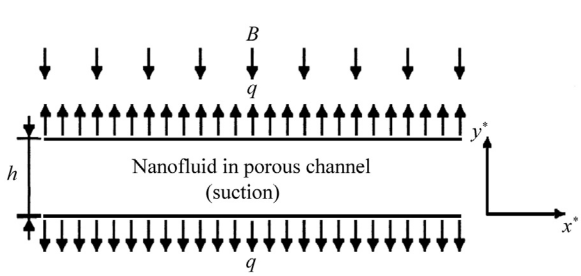

Figure 2 Schematic of the problem (nanofluid in a porous channel and magnetic field).

$$u^*\frac{\partial v^*}{\partial x^*}+v^*\frac{\partial v^*}{\partial y^*}=-\frac{1}{\rho_{nf}}\frac{\partial P^*}{\partial y^*}+\nu_{nf}\left(\frac{\partial^2 v^*}{\partial x^{*2}}+\frac{\partial^2 v^*}{\partial y^{*2}}\right), \tag{3}$$

$$\rho_{nf}C_p\left(u^*\frac{\partial T}{\partial x^*}+v^*\frac{\partial T}{\partial y^*}\right) = k_{nf}\left(\frac{\partial^2 T}{\partial x^{*2}}+\frac{\partial^2 T}{\partial y^{*2}}\right)+\mu_{nf}\left(\frac{\partial u^*}{\partial y^*}\right)^2. \tag{4}$$

The suitable boundary conditions for the velocity and temperature are:

$$y^*=0: \quad u^*=0, \quad T=T_0, \quad v^*=-q \tag{5}$$

$$y^*=h: \quad u^*=u_0, \quad T=T_h, \quad v^*=q \tag{6}$$

Calculating a mean velocity U by the relation:

$$U\times h=\int_0^h u^*\times dy^*=L_x\times q \tag{7}$$

We consider the following transformations:

$$x=\frac{x^*}{L_x},\quad y=\frac{y^*}{h},\quad u=\frac{u^*}{U},\quad v=\frac{v^*}{q},$$
$$P_y=\frac{P^*}{\rho q^2},\quad \theta=\frac{T-T_0}{T_h-T_0}. \tag{8}$$

Then, we can consider four dimensionless numbers: the Hartmann number Ha for the description of magnetic forces [11] and the Reynolds number Re for dynamic forces, Prandtl number and Eckert number:

$$Ha=Bh\sqrt{\frac{\sigma_f}{\rho_f\nu_f}}, \tag{9}$$

$$Re=\frac{hq}{\nu_{nf}} \tag{10}$$

$$Pr=\frac{\mu_{nf}C_p}{k_{nf}} \tag{11}$$

$$Ec=\frac{U^2}{C_p(T_h-T_0)} \tag{12}$$

where the effective density (ρ_{nf}) and specific heat capacity (C_p) are defined as [12]:

$$\rho_{nf}=\rho_f(1-\phi)+\rho_s\phi$$
$$(\rho C_p)_{nf}=(\rho C_p)_f(1-\phi)+(\rho C_p)_s\phi \tag{13}$$

The effective thermal conductivity of the nanofluid can be approximated by the Maxwell-Garnett's (MG) model as [13]:

$$\frac{k_{nf}}{k_f}=\frac{k_s+2k_f-2\phi(k_f-k_s)}{k_s+2k_f+\phi(k_f-k_s)} \tag{14}$$

where ϕ is the nanoparticle volume fraction. Different models for simulating dynamic viscosity of the nanofluids are shown in Table 1. In the first model, the effective thermal conductivity and viscosity of nanofluid are calculated by the Maxwell [13,35] and Brinkman models, respectively. The thermo physical properties of the nanofluid are given in Table 2.

Introducing Eqs. (7)-(12) into Eqs. (1)-(4) leads to the dimensionless equations:

$$\frac{\partial u}{\partial x}+\frac{\partial v}{\partial y}=0, \tag{15}$$

$$u\frac{\partial u}{\partial x}+v\frac{\partial u}{\partial y} = -\varepsilon^2\frac{\partial P_y}{\partial x}+\frac{\nu_{nf}}{hq}\left(\varepsilon^2\frac{\partial^2 u}{\partial x^2}+\frac{\partial^2 u}{\partial y^2}\right)-u\frac{Ha^2}{Re}\frac{B^*}{A^*}, \tag{16}$$

$$u\frac{\partial v}{\partial x}+v\frac{\partial v}{\partial y}=-\frac{\partial P_y}{\partial y}+\frac{\nu_{nf}}{hq}\left(\varepsilon^2\frac{\partial^2 v}{\partial x^2}+\frac{\partial^2 v}{\partial y^2}\right), \tag{17}$$

$$\frac{C^*}{D^*}Pr\left[Re\left(u\frac{\partial\theta}{\partial x}+v\frac{\partial\theta}{\partial y}\right)-Ec\left(\frac{\partial u}{\partial y}\right)^2\right] = \varepsilon^2\left(\frac{\partial^2\theta}{\partial x^2}+\frac{\partial^2\theta}{\partial y^2}\right). \tag{18}$$

where A^*, B^*, C^* and D^* are constant parameters:

$$A^*=(1-\phi)+\frac{\rho_s}{\rho_f}\phi,$$
$$B^*=1+\frac{3\left(\frac{\sigma_s}{\sigma_f}-1\right)\phi}{\left(\frac{\sigma_s}{\sigma_f}+2\right)-\left(\frac{\sigma_s}{\sigma_f}-1\right)\phi}. \tag{19}$$

Table 1 Different models for simulation of dynamic viscosity.

Model	Thermal conductivity	Dynamic viscosity
I	$\frac{\sigma_{nf}}{\sigma_f}=1+\frac{3(\frac{\sigma_s}{\sigma_f}-1)\phi}{(\frac{\sigma_s}{\sigma_f}+2)-(\frac{\sigma_s}{\sigma_f}-1)\phi}$	$\mu_{nf}=\frac{\mu_f}{(1-\phi)^{2.5}}$
II	$\frac{\sigma_{nf}}{\sigma_f}=1+\frac{3(\frac{\sigma_s}{\sigma_f}-1)\phi}{(\frac{\sigma_s}{\sigma_f}+2)-(\frac{\sigma_s}{\sigma_f}-1)\phi}$	$\mu_{nf}=\mu_f(1+7.3\phi+123\phi^2)$

$$C^*=\frac{k_s+2k_f-2\phi(k_f-k_s)}{k_s+2k_f+\phi(k_f-k_s)},$$
$$D^*=(1-\phi)+\frac{(\rho C_P)_s}{(\rho C_P)_f}\phi \tag{20}$$

Quantity of ε is defined as the aspect ratio between distance h and a characteristic length L_x of the slider. This ratio is normally small. Berman's similarity transformation is used to be free from the aspect ratio of ε:

$$v=-\ V(y),\quad u=\frac{u^*}{U}=u_0U(y)+x\frac{\mathrm{d}V}{\mathrm{d}y}. \tag{21}$$

Introducing Eq. (21) in the second momentum Eq. (17) shows that quantity $\partial P_y/\partial y$ does not depend on the longitudinal variable x. With the first momentum equation, we also observe that $\partial^2 P_y/\partial x^2$ is independent of x. We omit asterisks for simplicity. Then a separation of variables leads to [11]:

$$UV'-VU'=\frac{1}{Re}\frac{1}{A^*(1-\phi)^{2.5}}\left[U''-Ha^2B^*(1-\phi)^{2.5}U\right] \tag{22}$$

$$V^{IV}=Ha^2B^*(1-\phi)^{2.5}\ V'' +ReA^*(1-\phi)^{2.5}[V'\ V''-VV'''] \tag{23}$$

$$\theta''=-\frac{C^*}{D^*}(1-\phi)^{2.5}Pr\left(Re(1-\phi)^{2.5}V\theta'+Ec(u_0U')^2\right) \tag{24}$$

Where primes denote differentiation with respect to y and asterisks have been omitted for simplicity. The dynamic boundary conditions are:

$$y=0:\quad U=0,\ \ V'=0,\ \ \theta=0,\ \ V=1$$
$$y=1:\quad U=1,\ \ V'=0,\ \ \theta=1,\ \ V=-1 \tag{25}$$

3. Describe least square method and applied to the problem

3.1. Describe least square method

As Sheikholeslami, Hatami and Ganji [34] defined least square method is one of the weighted residual methods which are constructed on minimizing the residuals of the trial function introduced to the nonlinear differential

Table 2 Thermo physical properties of nanofluids and nanoparticles.

Material	Density/(kg/m^3)	Electrical conductivity/Ω	Specific heat capacity/(J/(kg·K))	Thermal conductivity/(W/(m·K))
Silver	10500	6.30×10^7	230	418
Copper	8933	5.96×10^7	385	401
Ethylene glycol	1113.2	1.07×10^{-4}	2410	0.252
Drinking water	997.1	0.05	4179	0.613

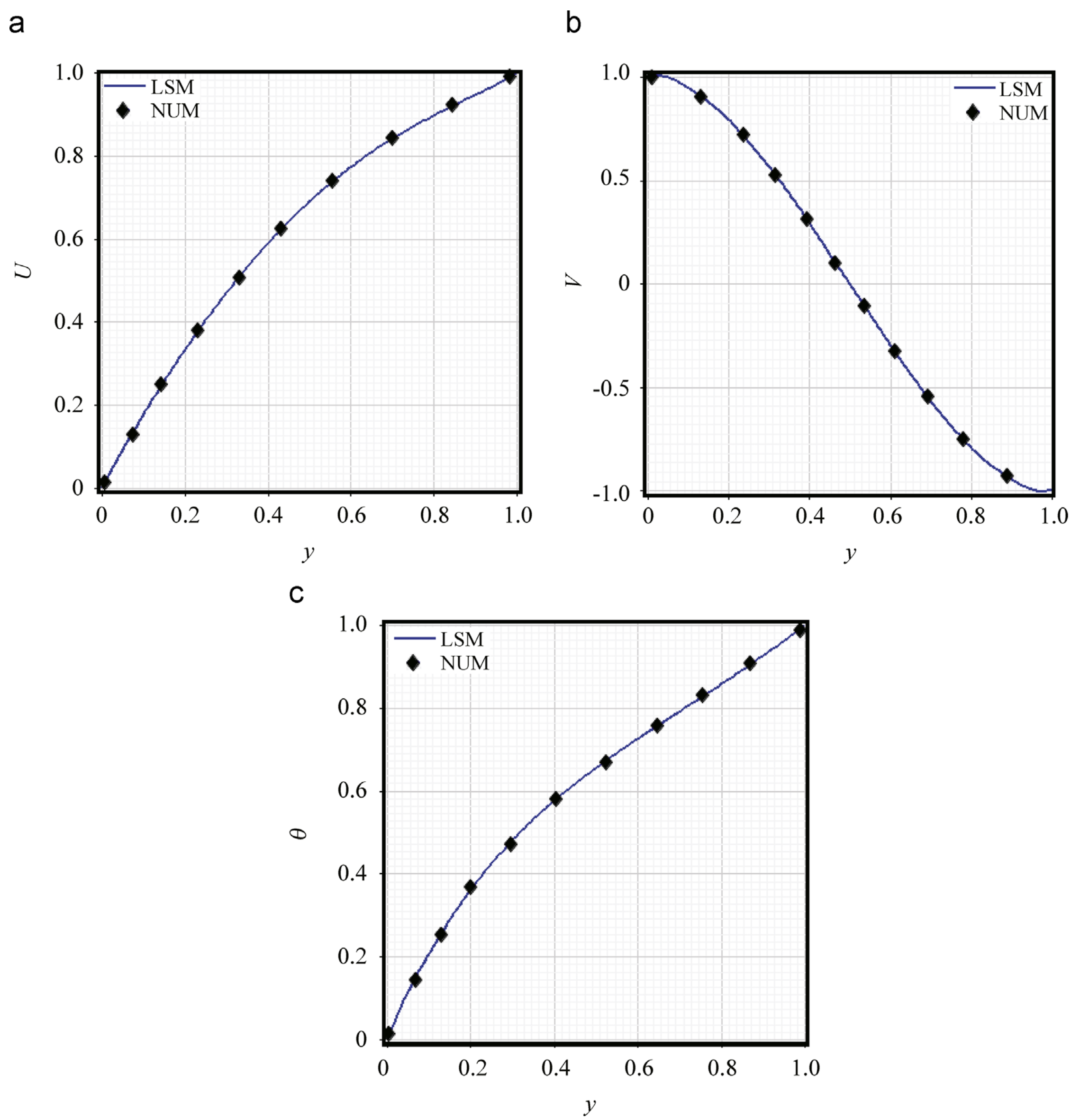

Figure 3 Comparison of LSM and numerical results for dimensionless velocities and temperature (water with copper, $Re=Ha=Ec=1$, $Pr=5.784$, $\varphi=0.04$). (a) $U(y)$, (b) $V(y)$ and (c) $\theta(y)$.

equation. For perception the principle of LSM, consider a differential operator D is acted on a function u to produce a function p:

$$D(u(x)) = p(x) \tag{26}$$

It is considered that u is estimated by a function, $\tilde{u}$ which is a linear combination of fundamental functions chosen from a linearly independent set. This is,

$$u \cong \tilde{u} = \sum_{i=1}^{n} c_i \varphi_i \tag{27}$$

By substituting Eq. (27) into the differential operator, D, the result of the operations generally isn't $p(x)$ and a difference will be appeared. Hence an error or residual will exist as follows:

$$R(x) = D(\tilde{u}(x)) - p(x) \neq 0 \tag{28}$$

The main concept of LSM is to force the residual to zero in some average sense over the domain. So,

$$\int_x R(x)\, W_i(x) = 0, \qquad i = 1, 2, \ldots, n \tag{29}$$

Where the number of weight functions W_i, is accurately equal the number of unknown coefficients c_i in $\tilde{u}$. The result is a set of n algebraic equations for the undefined coefficients c_i. If the continuous summation of all the squared residuals is minimized, the rationale behind the LSM's name can be seen. In other words, a minimum of

$$S = \int_x R(x)R(x)\mathrm{d}x = \int_x R^2(x)\mathrm{d}x \tag{30}$$

In order to achieve a minimum of this function Eq. (30), the derivatives of S with respect to all the each unknown

Table 3 Comparison between $V(y)$, $U(y)$ and $\theta(y)$ results from applied method for $Re=Ha=1$ and $\varphi=0.04$.

Y	LSM(U)	LSM(V)	LSM(θ)	NUM(U)	NUM(V)	NUM(θ)
0.00	0.000000000	1.0000000000	0.000000000	0.00000000	1.0000000000	0.000000000
0.05	0.090079318	0.99148600491	0.104436385	0.09007845	0.99148600324	0.1044361236
0.10	0.173699391	0.96310215552	0.1984024685	0.173698521	0.96310215127	0.1984024476
0.15	0.251233641	0.91204484837	0.2826882739	0.251232965	0.91204484587	0.2826882564
0.20	0.323055449	0.83727919592	0.3580838284	0.323054356	0.83727919265	0.3580838025
0.25	0.389538208	0.73931793883	0.4253791585	0.389537854	0.73931793652	0.4253791313
0.30	0.451055309	0.62000035523	0.4853642899	0.451054987	0.62000035327	0.4853642298
0.35	0.507980143	0.48227117125	0.5388292494	0.507980123	0.48227116987	0.5388292145
0.40	0.560686104	0.32995947166	0.5865640629	0.560685874	0.32995946852	0.5865640112
0.45	0.609546581	0.16755761079	0.6293587568	0.609546023	0.16755760954	0.6293587367
0.50	0.654934967	0.0000000000	0.6680033572	0.654934625	0.0000000000	0.6680033369
0.55	0.697224654	−0.1675573728	0.7032878909	0.697224423	−0.1675573256	0.7032878745
0.60	0.736789033	−0.3299592475	0.7360023827	0.736788821	−0.3299592145	0.7360023659
0.65	0.774001497	−0.4822709701	0.7669368607	0.774001124	−0.4822709564	0.7669368451
0.70	0.809235436	−0.6200001831	0.7968813502	0.809235123	−0.6200001628	0.7968813364
0.75	0.842864242	−0.7393178022	0.8266258782	0.842864023	−0.7393177639	0.8266258521
0.80	0.875261309	−0.8372790971	0.8569604690	0.875261207	−0.8372790847	0.8569604480
0.85	0.906800025	−0.9120447863	0.8886751507	0.906789651	−0.9120447541	0.8886751258
0.90	0.937853785	−0.9631021266	0.9225599496	0.937853569	−0.9631021023	0.9225599023
0.95	0.968795979	−0.9914860001	0.9594048899	0.968795741	−0.9914859213	0.9594048523
1.00	1.000000000	−1.0000000000	1.000000000	1.000000000	−1.0000000000	1.000000000

parameter should be zero. i.e.

$$\frac{\partial S}{\partial c_i} = 2\int_x R(x)\frac{\partial R}{\partial c_i}\mathrm{d}x = 0 \tag{31}$$

Comparing with Eq. (31), the weighted functions for LSM will be,

$$W_i = 2\frac{\partial R}{\partial c_i} \tag{32}$$

Because the "2" coefficient can be eliminated, it can be negligible in the equation. So the weighted functions, W_i, for the least squares method are the derivatives of the residuals with respect to the unknown constants

$$W_i = \frac{\partial R}{\partial c_i} \tag{33}$$

Many advantages of LSM compared to other analytical and numerical methods make it more valuable and motivate researchers to use it for solving heat transfer problems. Some of these advantages are listed below:

(a) It solves the equations directly and no simplifications needs. For example it solves power nonlinear terms without expanding or using Taylor expansion against differential transformation method (DTM).
(b) It does not needs to any perturbation, linearization or small parameter versus homotopy perturbation method (HPM) and parameter perturbation method (PPM).
(c) It is simple and powerful compared to numerical methods and reaches to final results faster than numerical procedures while its results are acceptable and have excellent agreement with numerical outcomes, furthermore its accuracy can be increased by increasing the statements of the trial functions.
(d) It does not needs to determining the auxiliary parameter and auxiliary function versus homotopy analysis method (HAM).

3.2. The LSM applied to the problem

It should be noted that the trial solution must satisfies the boundary conditions, so the trial solution can be written as

$$U(y) = y + c_1(y-y^2) + c_2(y-y^3) \tag{34}$$

$$V(y) = 1 + c_3\left(\frac{y^2}{2}-\frac{y^3}{3}\right) + c_4\left(\frac{y^2}{2}-\frac{y^4}{4}\right) + c_5\left(\frac{y^2}{2}-\frac{y^5}{5}\right) \tag{35}$$

$$\theta(y) = y + c_6(y-y^2) + c_7(y-y^3) \tag{36}$$

By introducing this equation to the Eqs. (22)-(24) residual function will be found and by substituting the residual function into Eqs. (34)-(36) a set of equations with seven equations and seven unknown coefficients will be appeared and by solving this system of equations, coefficients c_1-c_7 will be determined. By using LSM, when $Re=1$, $Ha=1$, $Pr=5.784$, $Ec=1$, $\varphi=0.04$, $u_0=1$, $A^*=1.318359242$, $B^*=1.125$, $C^*=1.124404794$ and $D^*=0.9930146705$ following equations will be determined for temperature distribution and velocities for laminar nanofluid flow in channel with permeable walls in the presence of a transverse magnetic field.

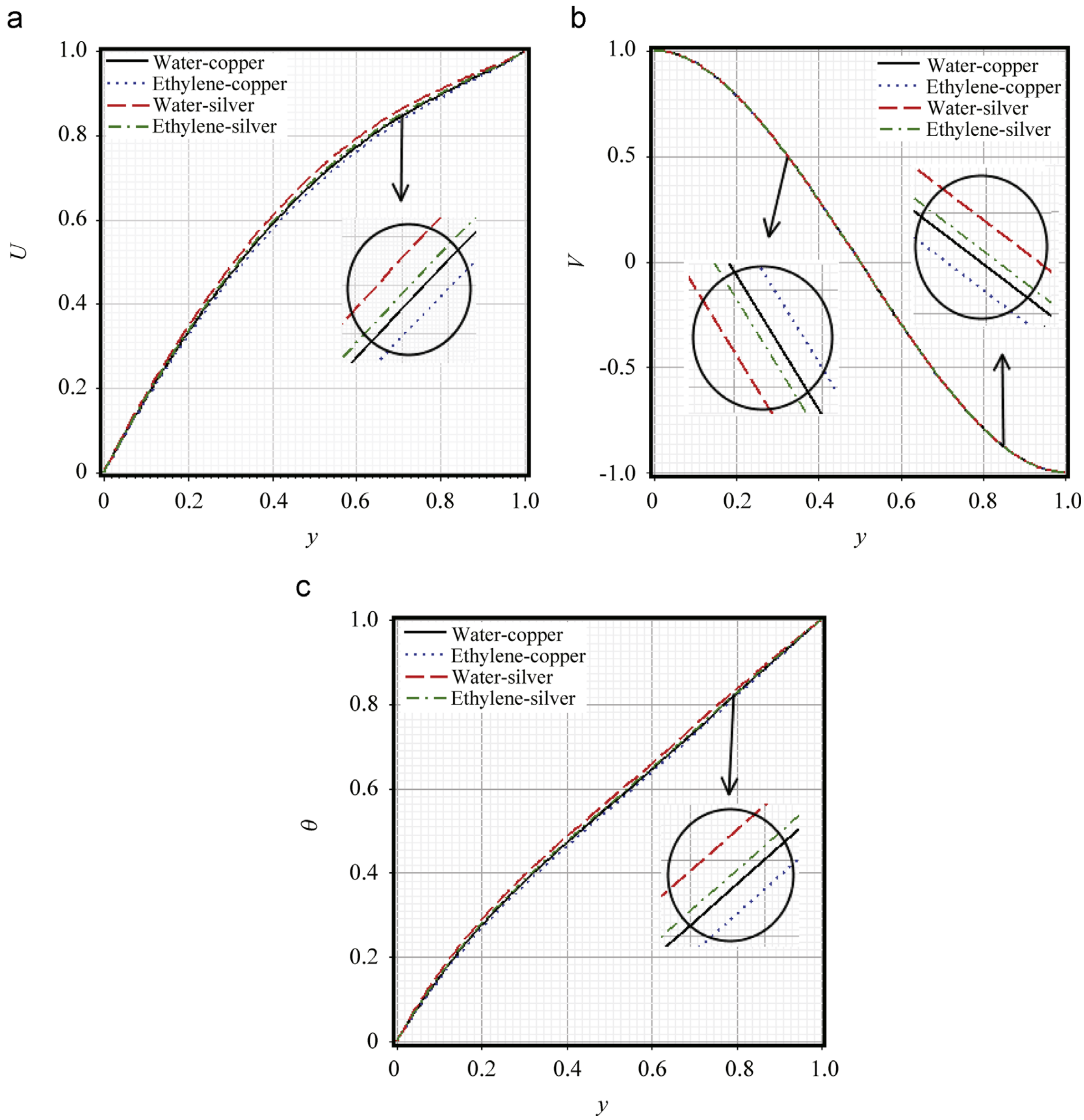

Figure 4 The effects of the nanoparticle and liquid phase material on velocity and temperature's profiles. ($Re=Ha=Ec=1$, $Pr=5.784$, $\varphi=0.04$).

$$U(y)=1.868667713y-1.366523314y^2+0.4978556007y^3 \tag{37}$$

$$V(y)=1-3.05213624y^2-7.791449777y^3+14.73930823y^4-5.895722226y^5 \tag{38}$$

$$\theta(y)=2.198697637y-2.252066004y^2+1.053368367y^3 \tag{39}$$

4. Results and discussion

In the present study LSM method is applied to obtain an explicit analytic solution of the laminar nanofluid flow and heat transfer in a channel with porous walls in the presence of uniform magnetic field (Figure 1). The numerical solution is performed using the algebra package Maple 18.0, to solve the present case. The software uses a second-order difference scheme combined with an order bootstrap technique with mesh-refinement strategies: the difference scheme is based on either the trapezoid or midpoint rules; the order improvement/accuracy enhancement is either Runge-Kutta fourth-rate or a method of deferred corrections.

First, in Figure 3 the comparison between the present method and numerical method to solve this problem for Cu-water nanofluid has been shown. Comparison between analytical and numerical methods for U, V and θ are provided in Table 3. As is observed the presented analytical method is a valid and powerful method to solve this kinds of problems in science and engineering. The effects of the nanoparticle and liquid phase material on velocity's profiles are shown in Figure 4. This figure reveals that when nanofluid includes silver (as nanoparticles) and water (as

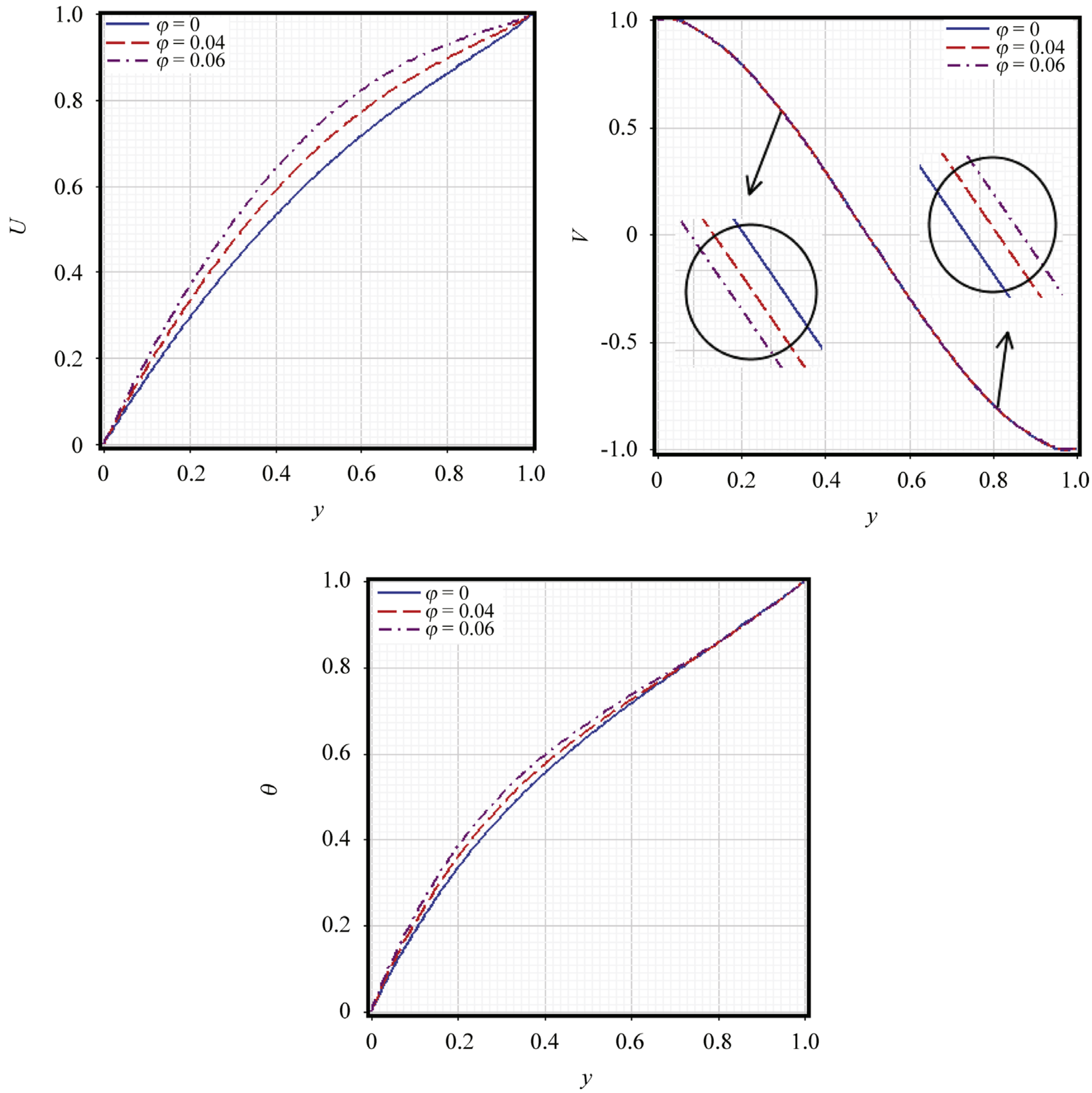

Figure 5 Effect of nanoparticle volume fraction, φ, on $U(y)$, $V(y)$ and $\theta(y)$, for water with copper nanoparticles when $Re=Ha=Ec=1$, $Pr=5.784$.

fluid phase) in its structure, the $U(y)$ and $\theta(y)$ values is greater than the other structures. Figure 5 shows the effect of nanoparticle volume fraction on $U(y)$, $V(y)$ and $\theta(y)$ for water with copper nanoparticles when $Re=Ha=Ec=1$, $Pr=5.784$. Nanoparticle volume fraction has no significant effect on velocity and temperature profiles and with the increasing volume fraction of the nanoparticles, the dimensionless boundary layer velocity and temperature increases. Effects of magnetic field on the temperature and velocity profiles are shown in Figure 6. Generally, when the magnetic field is imposed on the enclosure, the velocity field suppressed owing to the retarding effect of the Lorenz force. For example, when $Re=10$ is $U(y)$ will have the lowest. Also Hartmann number increases $V(y)$ decreases for $y<y_m$ but opposite trend is observed for $y<y_m$, y_m is a meeting point that all curves joint together at this point. At low Re and Ec, Ha increases for $y>y_m$ θ is increased, but for $y<y_m$ opposite is true. When Re and Ec are of great value, with increasing the Ha number, $\theta(y)$ is increasing. Effects of Reynolds number on the temperature and velocity profiles are shown in Figure 7. The velocity profile $V(y)$ is not affected by Reynolds number changes. For low Hartman number, as Reynolds number increases $U(y)$ is decreased. For high Hartman number, as Reynolds number increases $U(y)$ increases for $y<y_m$ but opposite trend is observed for $y>y_m$.

It is worth to mention that the Reynolds number indicates the relative significance of the inertia effect compared to the viscous effect and in turn increasing Re leads to an increase in the magnitude of the skin friction coefficient. For low Ha and Ec number, as Reynolds number increases temperature increases but for high Ha and Ec number opposite trend is observed. Effect of Prandtl number on the temperature profile is shown Figure 8. It may be concluded, the maximum value of θ in both a and b of nanofluids Ethylene-silver, and the maximum value of $\theta(y)$ for nanofluids Ethylene-silver at $Re=Ha=Ec=10$ will be. Figure 9

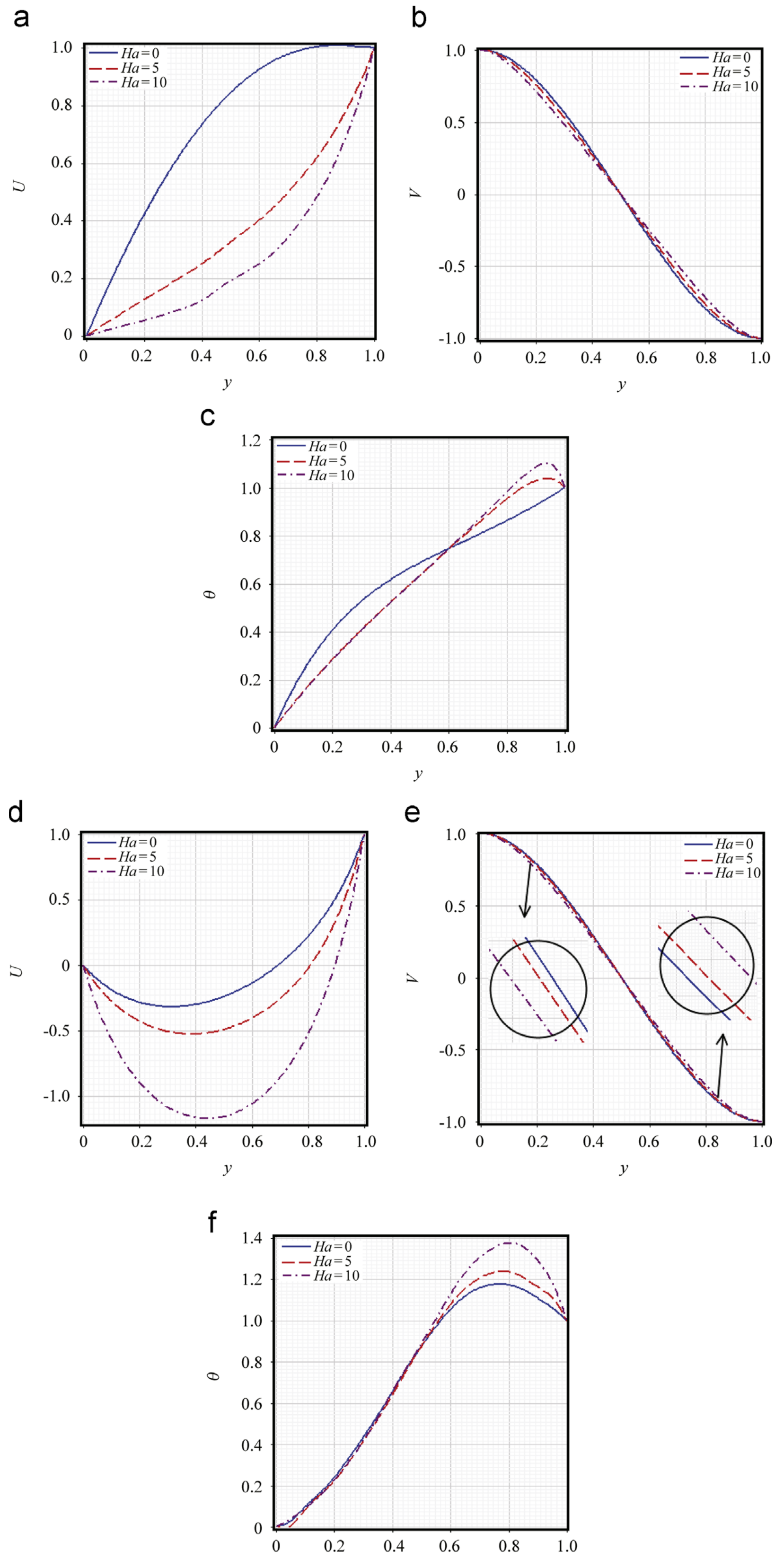

Figure 6 Effect of Hartmann number (Ha) on dimensionless velocities and temperature for water with copper nanoparticles, $\varphi=0.04$. (a) $V(y)$, $Re=1$, (b) $U(y)$, $Re=1$, (c) $\theta(y)$, $Re=Ec=1$, $Pr=5.784$, (d) $V(y)$, $Re=5$, (e) $U(y)$, $Re=5$, and (f) $\theta(y)$, $Re=Ec=5$, $Pr=5.784$.

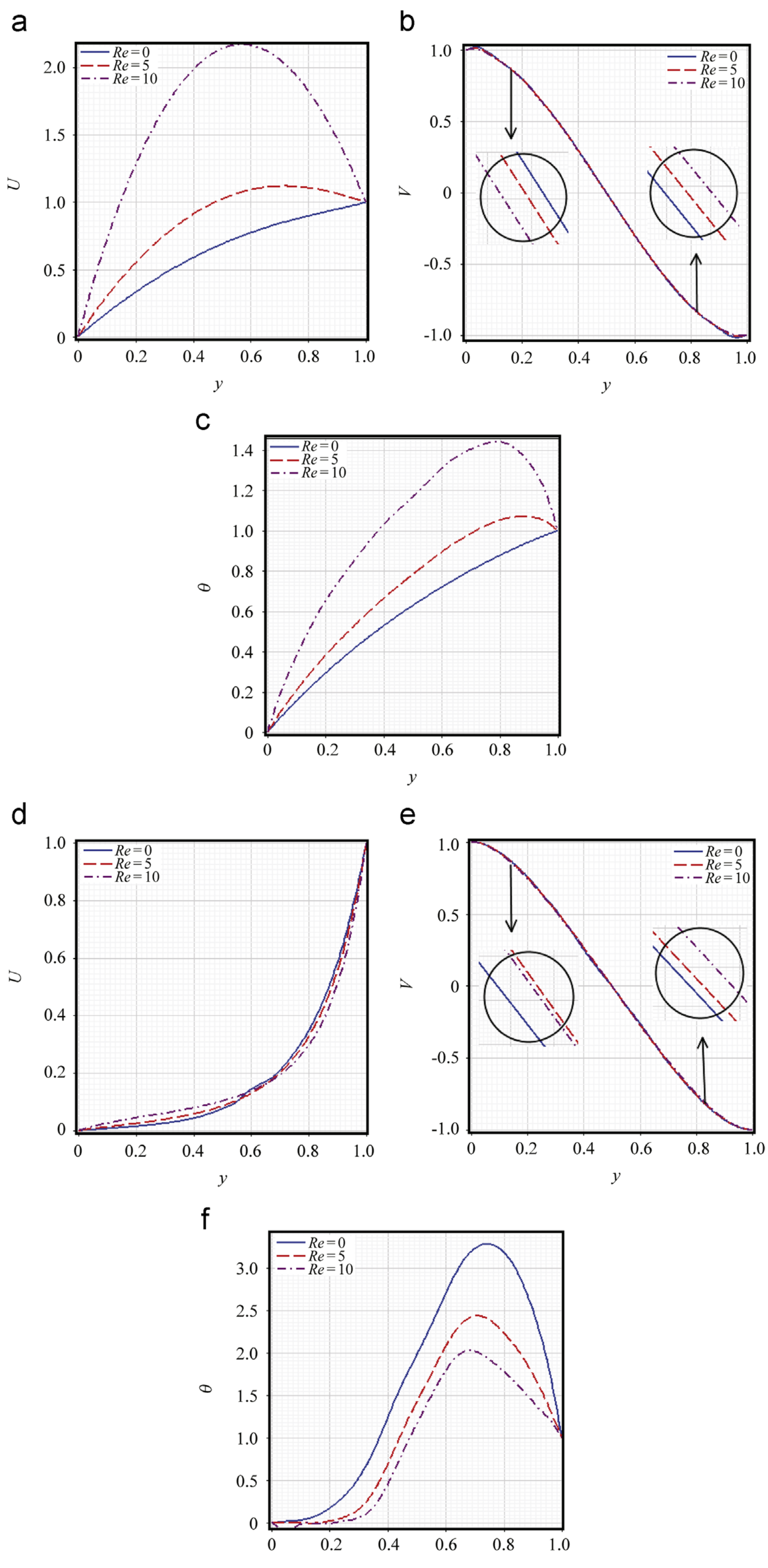

Figure 7 Effect of Reynolds number (Re) on dimensionless velocities and temperature for water with copper nanoparticles, $\varphi=0.04$. (a) $V(y)$, $Ha=1$, (b) $U(y)$, $Ha=1$, (c) $\theta(y)$, $Ha=Ec=1$, $Pr=5.784$, (d) $V(y)$, $Ha=10$, (e) $U(y)$, $Ha=10$, and (f) $\theta(y)$, $Ha=Ec=10$, $Pr=5.784$.

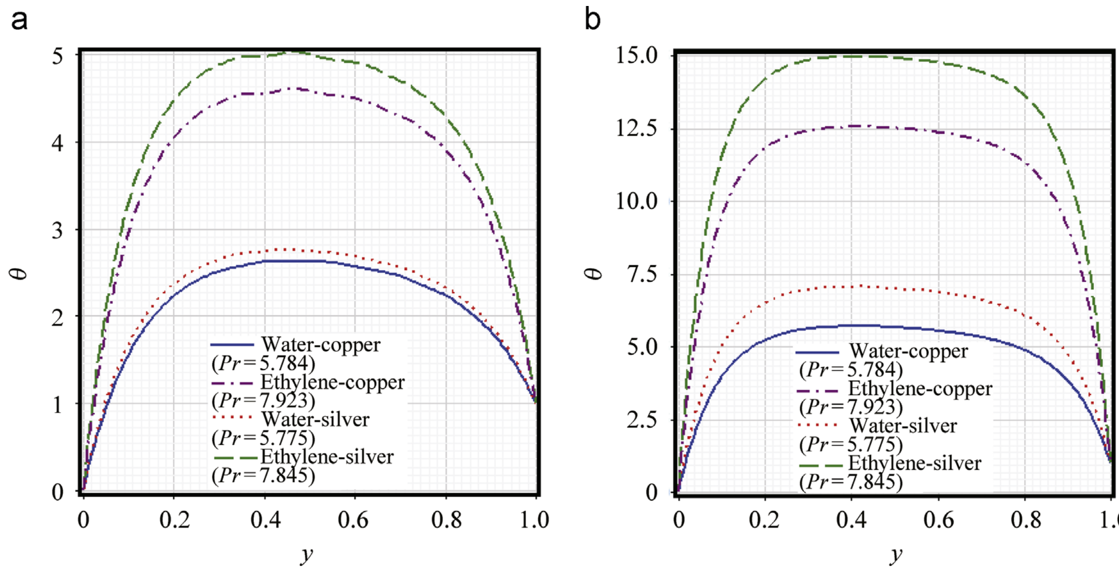

Figure 8 Effect of Prandtl number on dimensionless temperature for water with copper nanoparticles, $\varphi=0.04$. (a) $\theta(y)$, $Ha=Re=Ec=1$ and (b) $\theta(y)$, $Ha=Re=Ec=10$.

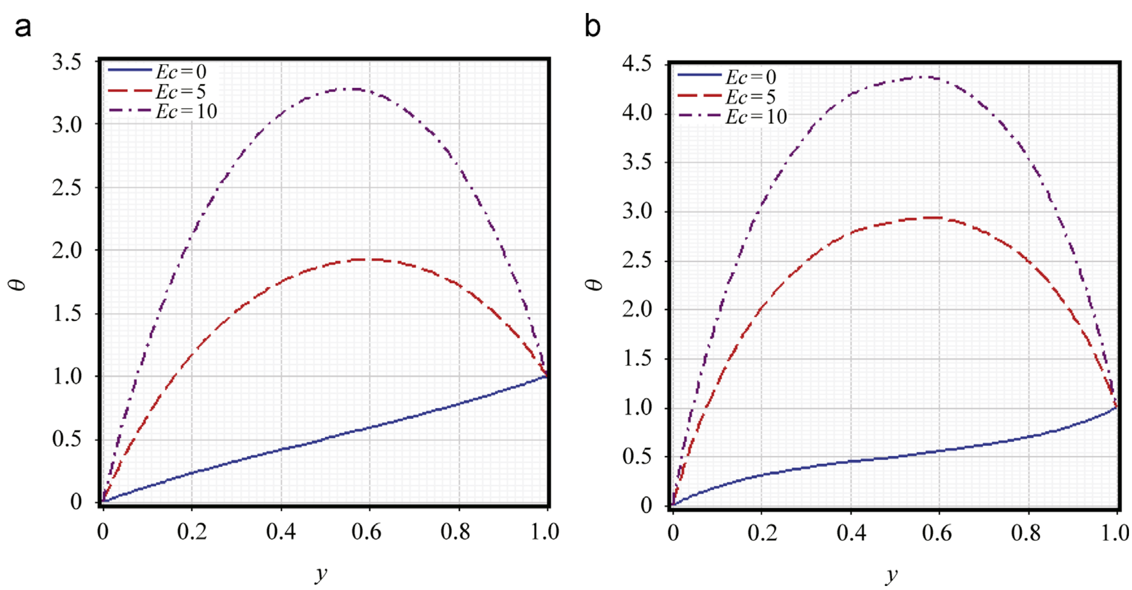

Figure 9 Effect of Eckert number on dimensionless temperature for water with copper nanoparticles, $\varphi=0.04$. (a) $\theta(y)$, $Ha=Re=1$, $Pr=5.784$ and (b) $\theta(y)$, $Ha=Re=10$, $Pr=5.784$.

shows the effects of Eckert number on the temperature profile. Generaly, increasing the Eckert number, the maximum value of theta increases and maximum value of θ occurs at $Ha=Re=10$. In all above result model I was used for simulating μ_{nf}. Figure 10 displays the temperature and velocity profiles for different models of μ_{nf}. This figure shows that selecting model II leads to smaller velocity boundary layer thickness and bigger temperature boundary layer thickness.

5. Conclusions

In this study, least square method (LSM) is applied to solve the problem of laminar nanofluid flow and heat transfer in a channel with porous walls in the presence of uniform magnetic field. First of all a comparison between the applied method, LSM and numerical method is investigated. The results indicate that least square method has a good agreement with numerically results. By solution of this equation the following points is concluded:

- In general, by applied magnetic field, velocity in the channel is reduced and the maximum amount of temperature increases.
- Increasing of Reynolds number increases the nanofluid flow velocity in the channel and also when the value of Hartmann and Eckert number is low, increasing the Reynolds number increases the maximum value of θ but when the value of Hartmann and Eckert is high,

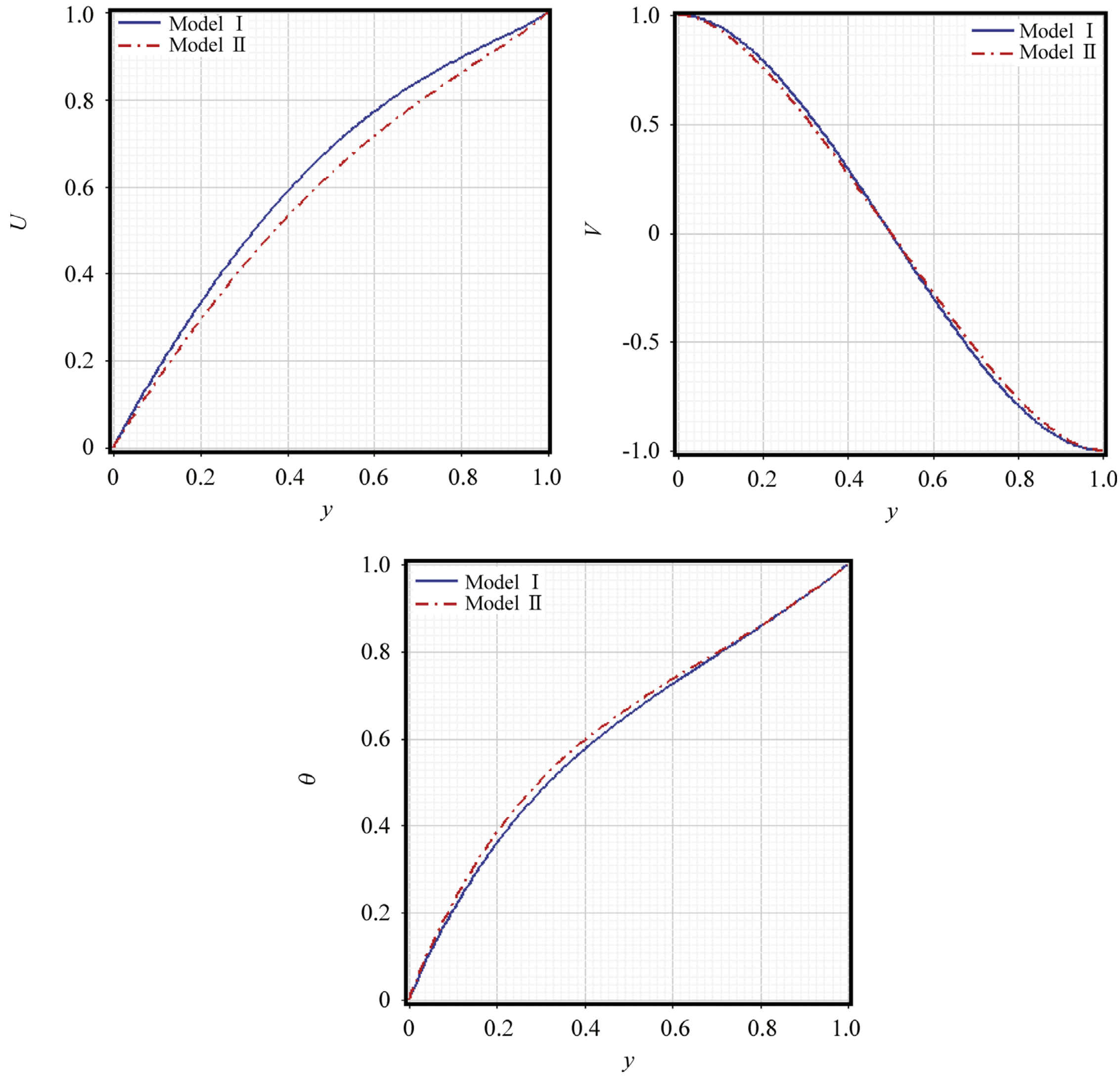

Figure 10 Velocity and temperature profiles for the different models for $Re = Ha = Ec = 1$, $Pr = 5.784$ and Cu-water case ($\varphi = 0.04$).

increasing the Reynolds number reduces the maximum value of θ.

In general, increasing of Prandtl and Eckert number increases the maximum value of θ when the Reynolds and Hartmann have a high quantity.

References

[1] V. Wernert, O. Schäf, H. Ghobarkar, R. Denoyel, Adsorption properties of zeolites for artificial kidney applications, Microporous Mesoporous Materials 83 (2005) 101–113.

[2] A. Jafari, P. Zamankhan, S.M. Mousavi, P. Kolari, Numerical investigation of blood flow, part II: in capillaries, Commun. Nonlinear Sci. Numer. Simul 14 (4) (2009) 1396–1402.

[3] A.R. Goerke, J. Leung, S.R. Wickramasinghe, Mass and momentum transfer in blood oxygenators, Chem. Eng. Sci. 57 (11) (2002) 2035–2046.

[4] S.S. Mneina, G.O. Martens, Linear phase matched filter design with causal real symmetric impulse response, AEU - Int. J. Electron. Commun 63 (2) (2009) 83–91.

[5] Y.H. Andoh, B. Lips, Prediction of porous walls thermal protection by effusion or transpiration cooling, an analytical approach, Appl. Therm. Eng. 23 (15) (2003) 1947–1958.

[6] A. Runstedtler, On themodified Stefan-Maxwell equation for isothermal multi component gaseous diffusion, Chem. Eng. Sci. 61 (2006) 5021–5029.

[7] A.S. Berman, Laminar flow in channels with porous walls, J. Appl. Phys. 24 (9) (1953) 1232.

[8] A.K.S.P. Chandran, N.C. Sacheti, Analyse the effects of a magnetic field on the thermodynamic flow past a continuously moving porous plate, Int. Commun. Heat Mass Transf 23 (1996) 889.

[9] M. Sheikholeslami, D. Domairry, H.R. Ashorynejad, I. Hashim, Investigation of the laminar viscous flow in a semi-porous channel in the presence of uniform magnetic field using optimal homotopy asymptotic method, Sains Malaysiana 41 (10) (2012) 1177–1229.

[10] S. Soleimani, M. Sheikholeslami, D.D. Ganji, M. Gorji-Bandpay, Natural convection heat transfer in a nanofluid

filled semi-annulus enclosure, Int. Commun. Heat Mass Transf 39 (2012) 565–574.

[11] M. Sheikholeslami, H.R. Ashorynejad, G. Domairry, I. Hashim, Flow and heat transfer of Cu-water nanofluid between a stretching sheet and a porous surface in a rotating system (pages), Hindawi Publ. Corp. J. Appl. Math. 2012 (2012) 18 (Article ID 421320).

[12] M.A.A. Hamad, I. Pop, A.I. Md Ismail, Magnetic field effects on free convection flow of a nanofluid past a vertical semi-infinite flat plate, Nonlinear Anal. Real World Appl 12 (3) (2011) 1338–1346.

[13] D. Domairry, H.R. Sheikholeslami, M. Ashorynejad, R. Subba, R. Gorla, M. Khani, Natural convection flow of a non-Newtonian nanofluid between two vertical flat plates, Nanoeng. Nanosyst 225 (2012) 115–122.

[14] M. Sheikholeslami, M. Gorji-Bandpay, D.D. Ganji, Magnetic field effects on natural convection around a horizontal circular cylinder inside a square enclosure filled with nanofluid, Int. Commun. Heat Mass Transf 39 (7) (2012) 978–986.

[15] M. Sheikholeslami, M. Gorji-Bandpy, D.D. Ganji, S. Soleimani, S.M. Seyyedi, Natural convection of nanofluids in an enclosure between a circular and a sinusoidal cylinder in the presence of magnetic field, Int. Commun. Heat Mass Transf 39 (9) (2012) 1435–1443.

[16] M. Sheikholeslami, D.D. Ganji, H.R. Ashorynejad, H.B. Rokni, Analytical investigation of Jeffery-Hamel flow with high magnetic field and nanoparticle by adomian decomposition method, Appl. Math. Mech. English Ed 33 (1) (2012) 25–36.

[17] M. Fakour, A. Vahabzadeh, D.D. Ganji, M. Hatami, Analytical study of micropolar fuid flow and heat transfer in a channel with permeable walls, Journal of Molecular Liquids 204 (2015) 198–204.

[18] M. Hatami, R. Nouri, D.D. Ganji, Forced convection analysis for MHD Al_2O_3-water nanofluid flow over a horizontal plate, Journal of Molecular Liquids 187 (2013) 294–301.

[19] M. Fakour, D.D. Ganji, M. Abbasi, Scrutiny of underdeveloped nanofluid MHD flow and heat conduction in a channel with porous walls, International Journal of Case Studies in Thermal Engineering 4 (2014) 202–214.

[20] A.V. Rosca, N.C. Rosca, T. Grosan, I. Pop, Non-Darcy mixed convection from a horizontal plate embedded in a nanofluid saturated porous media, Int. Commun. Heat Mass Transf 39 (8) (2012) 1080–1085.

[21] D.D. Ganji, M. Fakour, A. Vahabzadeh, S.H.H. Kachapi, Accuracy of VIM, HPM and ADM in solving nonlinear equations for the steady three-dimensional flow of a Walter's B fluid in vertical channel, Walailak Journal of Science and Technology 11 (7) (2014) 593–609.

[22] M. Fakour, A. Vahabzadeh, D.D. Ganji, Scrutiny of mixed convection flow of a nanofluid in a vertical channel, International Journal of Case Studies in Thermal Engineering 4 (2014) 15–23.

[23] A. Majidian, M. Fakour, A. Vahabzadeh, Analytical investigation of the Laminar viscous flow in a semi-porous channel in the presence of a uniform magnetic field, International Journal of Partial Differential Equations and Applications 2 (4) (2014) 79–85.

[24] A. Vahabzadeh, M. Fakour, D.D. Ganji, I. Rahimi Petroudi, Analytical accuracy of the one dimensional heat transfer in geometry with logarithmic various surfaces, Cent. Eur. J. Eng 4 (2014) 341–355.

[25] A. Vahabzadeh, M. Fakour, D.D. Ganji, Study of MHD nanofluid flow over a horizontal stretching plate by analytical methods, International Journal of Partial Differential Equations and Applications 2 (6) (2014) 96–104.

[26] M.N. Ozisik, Heat Conduction, Second edition, John Wiley & Sons Inc, USA, 1993.

[27] M. Hatami, D.D. Ganji, Heat transfer and nanofluid flow in suction and blowing process between parallel disks in presence of variable magnetic field, Journal of Molecular Liquids 190 (2014) 159–168.

[28] M. Hatami, J. Hatami, D.D. Ganji, Computer simulation of MHD blood conveying gold nanoparticles as a third grade non-Newtonian nanofluid in a hollow porous vessel, Computer Methods and Programs in Biomedicine 113 (2014) 632–641.

[29] G. Domairry, M. Hatami, Squeezing Cu-water nanofluid flow analysis between parallel plates by DTM-Padé method, Journal of Molecular Liquids 193 (2014) 37–44.

[30] Laminar flow and heat transfer of nanofluid between contracting and rotating disks by least square method, Powder Technology 253 (2014) 769–779.

[31] Natural convection of sodium alginate (SA) non-Newtonian nanofluid flow between two vertical flat plates by analytical and numerical methods, Case Studies in Thermal Engineering 2 (2014) 14–22.

[32] M. Sheikholeslami, M. Hatami, D.D. Ganji, Micropolar fluid flow and heat transfer in a permeable channel using analytical method, Journal of Molecular Liquids 194 (2014) 30–36.

[33] A. Desseaux, Influence of a magnetic field over a laminar viscous flow in a semi-porous channel, Int. J. Eng. Sci. 37 (1999) 1781–1794.

[34] M. Sheikholeslami, M. Hatami, D.D. Ganji, Analytical investigation of MHD nanofluid flow in a semi-porous channel, Powder Technology 246 (2013) 327–336.

[35] J.C. Maxwell, A Treatise on Electricity and Magnetism, Second edition, Oxford University Press, Cambridge, 1904, pp. 435-441.